POWER LOSS THROUGH DECORATIVE ELEMENTS IN THE FRONT GLAZING OF BIPV MODULES

Max Mittag, Christoph Kutter, Matthieu Ebert, Helen Rose Wilson, Ulrich Eitner
Fraunhofer Institute for Solar Energy Systems ISE
Heidenhofstr. 2, 79110 Freiburg, Germany
max.mittag@ise.fraunhofer.de

ABSTRACT: Printed module front covers can be designed to mask the geometry of solar cells for Building-Integrated Photovoltaics (BiPV). Such prints reduce the transmittance of the module front layer, which decreases module power. We performed transmittance measurements with large-area and small-area measurement equipment (220 mm / 620 mm integrating sphere) on different samples and find measurements applying small-area illumination to result in lower transmittance ($\Delta = 3.1_{abs}$% at 40% coverage) due to lateral losses in the samples. By measuring the power of modules with different design prints we find that the results do not correspond to transmittance measurements of the glass covers alone, even if a large-area transmittance measurement setup is used ($\Delta = 16\%_{abs}$ at 40% coverage). We attribute the differences between optical and electrical measurements to module internal reflection, optical coupling of the solar cell, partial transmittance by coatings and diffuse scattering of decorative prints. Differences increase with the share of coated glass area. We perform electrical and LBIC measurements on modules with printed and unprinted reference glass covers and calculate the effective transmittance. Short circuit currents calculated by spatial integration of LBIC results are in good agreement with results from I_{SC} measurements. We predict the effective transmittance for arbitrary prints based on selected I_{SC} measurements and find them to be in good agreement to measurements. In conclusion, we find transmittance measurements on printed glass alone to be insufficient to predict the optical power losses as they overestimate the optical loss.

Keywords: Building Integrated Photovoltaic Module, BiPV, CTM, Cell-to-Module, Power Prediction

1 INTRODUCTION

The European directive 2010/31/EU (nearly zero energy buildings) encourages the large-scale deployment of Building-Integrated Photovoltaics (BiPV) [1]. Yet today, BiPV market penetration is still low. One reason is that the aesthetic appearance of the photovoltaic components does not satisfy the expectations of architectural design. To overcome this, many efforts are being undertaken to conceal the photovoltaic components such as the individual PV cells or cell interconnectors and to give the PV modules a homogeneous appearance [2]-[5]. A very promising concept that meets the aesthetic demands of building integrated photovoltaics (BiPV) is to completely coat the front cover material with optically active layers (Figure 1). Another option is the printing of patterns that only cover parts of the front interface (i.e. geometric patterns of dots etc. (Figure 2).

Figure 1: Full-area coating of module front glass cover [11]

The drawback of such printed decorative patterns is the reduction of transmittance, thus decreasing the nominal module power and finally increasing the financial barrier and return on investment.

Gains and losses in common photovoltaic modules are well understood and models exist to predict module power and cell-to-module losses under Standard Testing Conditions (STC) [6]-[9]. The effects of additional decorative elements have been investigated by Frontini [10], quantifying the difference between camouflage coverage and module power loss that result from wave-optical effects.

Figure 2: Partial coating of front glass cover with dot pattern

2 METHOD

Decorative elements applied to the module front cover (usually a glass pane) affect the module power by increasing reflection (1) and additional absorption (2), which both lead to shading losses (Figure 3).
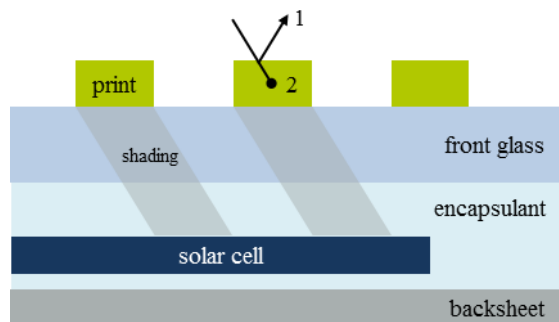
Figure 3: Schematic drawing of changes in module optics by application of decorative prints onto the module front cover

We analyze the effects of printed ceramic elements on the front glazing on module power. Transmittance

measurements using samples with different printed patterns and coverage are performed. We compare the results of small-area and large-area transmittance measurement configurations. Furthermore, we characterize the ceramic print patterns using surface profilometry, microscope imaging and light-beam induced current (LBIC) measurements.

We compare the projected power of a module with coated glass based on geometrical coverage of the printed coating, based on transmittance measurement results as well as based on measurements using laser-beam induced current (LBIC) on manufactured module samples. In addition, we perform power measurements on the module samples. Results of the electrical and optical measurements are compared and discussed.

a.   Geometric Coverage Ratio

Assuming complete opacity of the printed element, i.e. the print has zero transmittance; the ratio of the footprint of the design element to the total module is defined as the geometrical coverage ratio:

$$\mathrm{CR}_{geometrical} = \frac{\mathrm{A}_{decorative\,element}}{\mathrm{A}_{module}} \qquad (I)$$

While total opacity is a first-order assumption which is seldom valid in practice, the coverage ratio is nonetheless an important parameter as it represents a target value for production and dimensioning.

b.   Optical Measurements of Glass

We perform optical measurements on front glasses and modules with different geometrical coverage ratios. White dots are printed onto a set of glass samples using a digital ink jet printer and ceramic based ink. The targeted geometrical coverage ratio is 10%, 20% and 40%. An unprinted reference glass pane is available (Figure 4).
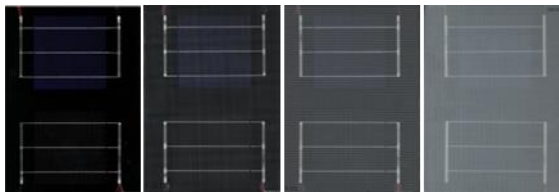
Figure 4: Photographs of mini-modules with covers made of digitally printed glass samples with different coverage ratios and reference glass pane. From left to right: Reference glass, 10% coverage ratio, 20% coverage ratio, 40% coverage ratio; small dots are printed

The glass samples are optically characterized using two different measurement setups. Method A uses a small-area light source and a small integrating sphere (diameter 220 mm). Method B uses a large integrating sphere (diameter 620 mm) with large-area illumination of the sample. It is widely accepted that a large aperture area and a large-area collimated radiation source are necessary to measure the transmittance of light-scattering, translucent materials accurately [12]-[14].

In Figure 5, the transmittance spectra of the different glass samples are shown. The effect of the two different characterization methods is reflected in the measured transmittance differences.

In Table 1 the measured transmittance values are shown, which are obtained by weighting the measured spectra by the AM1.5g spectrum and the spectral response of the solar cells that are used for prototype production.

The unprinted glass samples ($CR_{geometrical} = 0\%$) also features reflection and absorption. We calculate a relative transmittance ($T_{opt,\ rel}$) for both measurement setups which is relative to the transmittance of the unprinted glass sample.

The small-area illumination method (A) clearly underestimates the transmittance for higher coverage ratios, as expected. The differences between both measurement configurations increases with the coverage ratio ($3.1\%_{abs}$ at $CR_{geometrical} = 40\%$). For further consideration, the results from measurement B (large area) are therefore used.

The decrease of transmittance is not proportional to the increase of coverage. For example at 40% coverage, transmittance is still larger than 60%, showing that the geometrical coverage ratio alone is insufficient for predicting the power of a printed BiPV module.

Table 1: Average transmittance for different samples and characterization techniques, weighted with AM1.5g spectrum and spectral response of the solar cell used

$CR_{geometrical}$	0%	10%	20%	40%
$T_{opt.A}$	90.81%	82.32%	72.87%	58.32%
$T_{opt,A,rel}$	100%	90.7%	80.2%	64.2%
$T_{opt,B}$	90.56%	82.19%	74.35%	60.95%
$T_{opt,B,rel}$	100%	90.8%	82.1%	67.3%
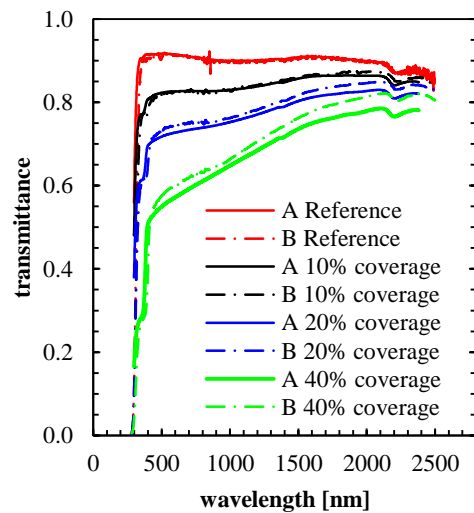
Figure 5: Transmittance spectra of glass samples covered with decorative elements (white dots), small (A) and large-area (B) illumination measurement setup, no additional weighting

Differences between geometrical coverage and transmittance measurement arise from a partial transparency of the decorative prints (3) as well as from scattering effects (4) as displayed in Figure 6. Shading of the solar cell (Figure 3) is replaced by reduced

transmittance (Figure 6, 3 and 5). Scattering causes increased path lengths within the front glass that leads to additional attenuation of light. Within both optical measurement configurations, the transmittance of the glass samples is measured against air. Therefore light that is redirected by more than approx. 42° by scattering in the ceramic print undergoes internal (total) reflection at the glass/air boundary (5). As a result, increased attenuation as well as light redirection to the sides of the glass samples decreases the measured transmittance at the sensor. In the large-area illumination configuration, however, lateral losses are largely compensated by lateral gains.
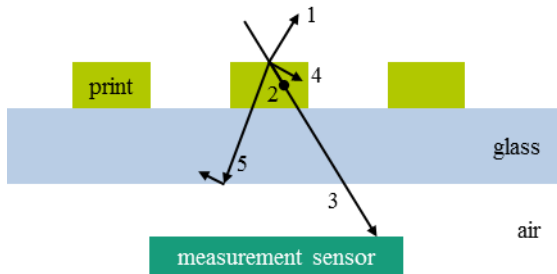
Figure 6: Schematic drawing of causes for differences between geometrical coverage and transmittance

c.   Characterization of Printed Elements

We record microscope images of different coating elements and measured the size of the prints (example shown in Figure 7). The images show that the desired geometrical coverage does not equal the actual geometric coverage due to jagged edges and over-/underprinting.
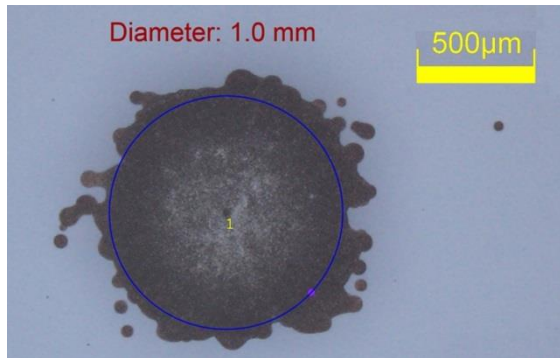
Figure 7: Microscope image of a printed dot

We perform a surface scan and find the thickness of printed elements to be inhomogeneous (Figure 8). Since the printed ink is partially transparent, the variation in thickness leads to spatially non-uniform transmittance of the printed element. We perform LBIC measurements on modules with printed glass and obtain spatially resolved information on module short circuit current. LBIC confirms the non-uniform transmittance of the printed elements (Figure 10).

Also the printed area features a rough surface, which leads to light scattering in transmission and reflection.
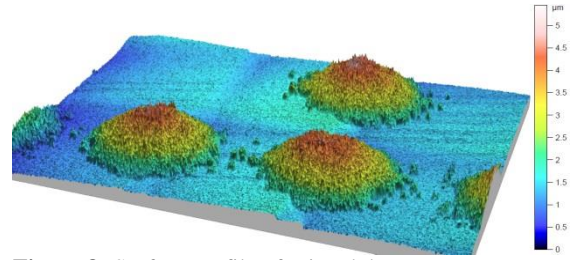
Figure 8: Surface profile of printed dots

We conclude that the geometrical coverage ratio is not a sufficient description of a print and that the coverage ratio may not be used as the sole basis for estimating the effective transmittance.

d.   Power Measurements on Modules with Partially Printed Glass Covers

After measuring the transmittance of glass samples with different coverage ratios, we prepare mini-module samples (Figure 4) and measure electrical module parameters. For each sample, an IV measurement with a flash simulator is performed at the Fraunhofer ISE CalLab PV Modules under standard testing conditions (STC).

We find the short circuit current (I_{SC}) to deviate from the values which were estimated based on geometrical coverage. Current measurements also deviate from predictions based on transmittance measurements (Table 2). Increased coverage of the front glass cover does not translate into equivalently decreased current.

Table 2: Measured short circuit currents

| $CR_{geometrical}$	0%	10%	20%	40%
$T_{opt,B,rel}$	100%	90.76%	82.10%	67.31%
$I_{sc,rel}$	100%	95.20%	89.20%	82.10%
$I_{sc,rel}$ - $T_{opt,B,rel}$	0%	4.4%	7.1%	14.8%

Performing measurements of the module power, similar results are obtained (Table 3). The difference between the geometrical coverage ratio and expected power is even higher than for the short circuit current. The increased module power (P_{MPP}) in comparison to the short circuit current is caused by a better fill factor, due to a lower current. We find the difference between power and transmittance measurements to be significant. At 40% coverage a difference of $16\%_{abs}$ between transmittance and normalized power is found.

Table 3: Measured module power

| $CR_{geometrical}$	0%	10%	20%	40%
$T_{opt,B,rel}$	100%	90.76%	82.10%	67.31%
$P_{MPP,rel}$	100%	95.90%	90.20%	83.60%
$P_{MPP,rel}$ - $T_{opt,B,rel}$	0%	5.1%	8.1%	16.3%

In addition to our previous findings, we conclude that transmittance measurements on the glass samples alone are insufficient for predicting BiPV module power for increased coverage ratios. Differences between the setups for transmittance measurement (Figure 6) and module power measurement (Figure 9) arise from coupling gains [6] to the solar cell within the module (Figure 9, 7). Figure 9 also shows increased incidence of light on the cell surface through additional gains by

internal reflection (6). Furthermore, the losses from reflection on position 2 of the front glass (inner interface) are reduced within the module (5) compared to the transmittance measurement, since the front glass and conventional encapsulation materials feature very similar refractive indices.
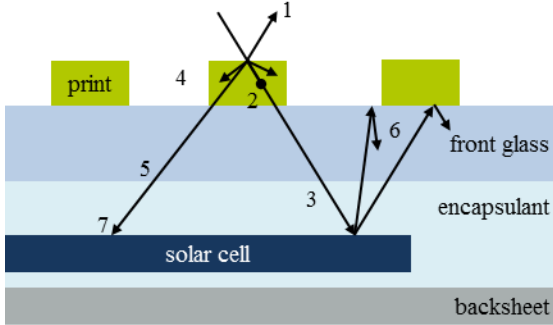
Figure 9: Schematic drawing of causes for differences between transmittance measurements and power measurements

In order to locally investigate the optical losses of the pattern with respect to cell current, we perform measurements on partially printed modules using laser-beam induced current (LBIC) and measure the external quantum efficiency (EQE) at five different wavelengths. On an area of 5x5 mm², 200x200 single spot measurements are performed. Samples with coverage ratios of 30% and 60% are measured. Using the EQE data from the LBIC measurements we compute the spatially resolved short circuit current (Figure 10).
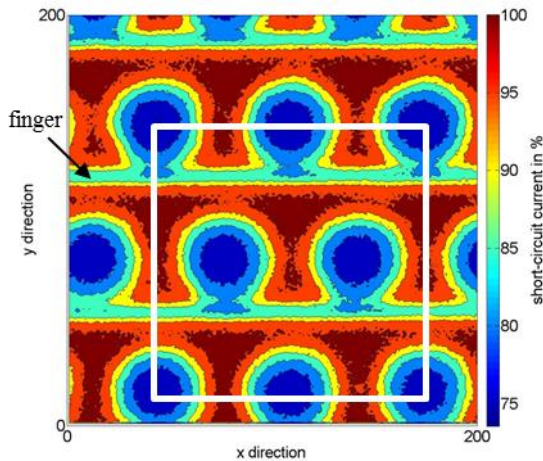
Figure 10: LBIC measurement results, spatially resolved relative short circuit current of a 1 mm white dot pattern. The area for spatial integration is outlined in white.

Horizontal lines in Figure 10 are due to the cell metallization (fingers).

We use a repeating area element (Figure 10, white square). By integrating over that area, we gain an effective value for short circuit current that includes the effects of scattering, and multiple reflections. It automatically weights the values for the printed and unprinted areas, analogous to the approach taken in [15, Annex C].

The integration over a defined area of the LBIC I_{SC} matrix is performed for the printed glass as well as for an unprinted reference. Both integrations are necessary to calculate the effective transmittance of the printed glass without additional effects of the cell metallization.

$$t_{eff,print} = \frac{\int_{x_{min,n}}^{x_{max,n}} \int_{y_{min,n}}^{y_{max,n}} I_{sc,norm} dx dy}{\int_{x_{min}}^{x_{max}} \int_{y_{min}}^{y_{max}} I_{sc,norm,Reference} dx dy} \quad \text{(II)}$$

We calculate the effective transmittance of printed front glass covers with different coverage ratios based on LBIC measurements performed on two different samples with coverage ratio of 30% and 60% (Figure 11, green square and red triangle, respectively). We find the calculated transmittance based on LBIC to be in good agreement with the transmittances based on the results of I_{SC} measurements ($\Delta < -0.37\%$ abs.).

A prediction of the effective transmittance and thus of the module power for arbitrary coverage ratios is therefore possible based on two LBIC measurements.

Although a prediction of the effective transmittance based on LBIC measurements is possible, a prediction based on I_{SC} measurements is a simpler alternative, since both measurements require module prototypes and IV measurement equipment is widely available.

We calculate the effective transmittance of arbitrary coverage ratios (Figure 11, blue line) based on two I_{SC} measurements at 30 and 60% coverage (blue squares) and find them to be in good agreement with measured values (black squares; MSE = 0.59%$_{abs}$). While this procedure can be used to estimate the effective transmittance for different coverage ratios of the same print element, it requires module samples with two different coverage ratios of the same print element.
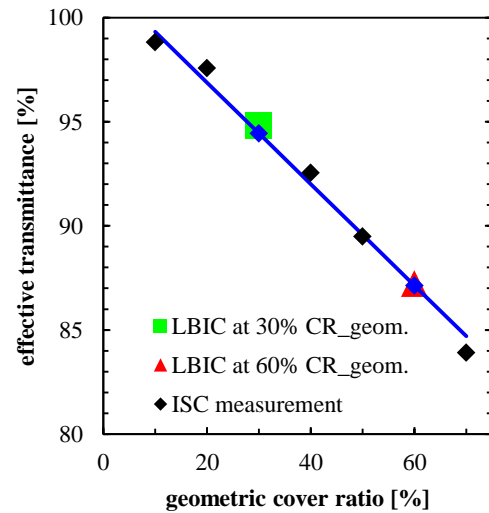
Figure 11: Calculation of the effective transmittance of printed front glass based on I_{SC} measurements on module samples with 30 and 60% coverage ratio versus measurements at other coverage ratios; effective transmittance calculated from LBIC measurements performed on samples with 30% (large green square) and 60% coverage ratio (large red triangle)

3 SUMMARY

Losses in common photovoltaic modules are well understood and models exist to predict module power. Effects of additional decorative elements have not yet been fully investigated. We analyze the effects in modules with printed front glass covers.

We perform electrical measurements on modules with different coverage ratios of printed elements. We find that the decrease in electrical power is not proportional to the increase in coverage ratio. The short circuit current is higher than expected, based on the degree of geometrical coverage alone.

We characterize the design prints by performing surface profilometry, microscope images and LBIC measurements. We find them to be non-homogeneous in thickness and also find their actual area to be different from the nominal size. LBIC images demonstrate that their transmittance is non-uniform.

We therefore conclude that the geometrical coverage ratio alone is not suitable for predicting module power or the effective transmittance of the printed glass.

We made transmittance measurements on glass that features design prints with different coverage ratios. Measurements were performed using illumination of small as well as large areas and with small (220 mm) as well as with large (620 mm) integrating spheres. We find the difference between the two measurement configurations to increase with the coverage ratio of the decorative print and the large-area measurements to result in higher transmittance values ($\Delta = 3.1_{abs}\%$ at 40% coverage). While transmittance measurements of the glass panes alone include effects of imperfect prints and partial transparency, they obviously cannot take effects of optical coupling to solar cells in modules into account. Correspondingly, results of transmittance measurement and power measurements do not agree ($\Delta = 16\%_{abs}$ at 40% coverage). We conclude that the use of transmittance value of the glass alone is also insufficient to predict the module power.

We calculate the effective transmittance of glass panes with arbitrary coverage ratios based on selected LBIC measurements as well as on I_{SC} measurements and find them to be in good agreement with comparative IV measurements. A prediction of module power is therefore possible based on selected measurements on single module prototypes.

We made LBIC measurements on module samples with selected coverage ratios and calculated the effective transmittance of the printed glass in the module. We used this information to predict the transmittance for different coverage ratios. Transmittance calculated using spatially integrated LBIC is close to results from electrical measurements of the complete module and allows spatially resolved analysis of optical effects resulting from prints.

4 ACKNOWLEDGEMENTS

5 REFERENCES

[1] European Parliament, "*Directive 2010/31/EU of the European Parliament and of the Council of 19 May 2010 on the energy performance of buildings*" http://data.europa.eu/eli/dir/2010/31/oj

[2] Verberne, G., et al, "*BIPV Products For Façades And Roofs: A Market Analysis*", 29th European PV Solar Energy Conference and Exhibition, 2014

[3] Scognamiglio, A., et al, "*Chapter 6 - Building-Integrated Photovoltaics (BIPV) for Cost-Effective Energy-Efficient Retrofitting*" Cost-Effective Energy Efficient Building Retrofitting: Woodhead Publishing, 2017, pp. 169–197

[4] Ferrara, C., et al, "*8 - Building-integrated photovoltaics (BIPV) A2 - Pearsall, Nicola,*" The Performance of Photovoltaic (PV) Systems, T1 - 8 - Building-integrated photovoltaics (BIPV) A2 - Pearsall, Nicola, Ed.: Woodhead Publishing, 2017, pp. 235–250

[5] Yang, T., et al, "*A review of research and developments of building-integrated photovoltaic/thermal (BIPV/T) systems*" Renewable and Sustainable Energy Reviews, vol. 66, pp. 886–912, 2016

[6] Haedrich, I., et al, "*Unified methodology for determining CTM ratios: Systematic prediction of module power*", Solar energy materials and solar cells 131 (2014), pp.14-23, ISSN: 0927-0248, SiliconPV, 2014

[7] Mittag, M., et al, "*Systematic PV module optimization with the cell-to-module (CTM) analysis software*", Photovoltaics International, vol. 36, 2017

[8] Mittag, M., et al, "*Electrical and Thermal Modeling of Junction Boxes*", 33rd European PV Solar Energy Conference and Exhibition, 2017

[9] Mittag, M., et al, "*Cell-to-Module (CTM) Analysis for Photovoltaic Modules with Shingled Solar Cells*", 44th IEEE Photovoltaic Specialists Conference, 2017

[10] Frontini, F., et al, "*Indoor And Outdoor Characterization Of Innovative Colored BIPV Modules For Façade Application*", 32nd European PV Solar Energy Conference and Exhibition, 2016

[11] Bläsi, B., et al, "*Morpho Butterfly Inspired Coloured BIPV Modules*", 33rd European PV Solar Energy Conference and Exhibition, 2017

[12] Chevalier, B., et al, "*Solar energy transmittance of translucent samples: A comparison between large and small integrating sphere measurements*" Solar Energy Materials and Solar Cells, vol. 54, no. 1–4, pp. 197–202, 1998

[13] Platzer, W. J., "*Directional-hemispherical solar transmittance data for plastic honeycomb-type structures*" Transparent insulation, vol. 49, no. 5, pp. 359–369, 1992

[14] Milburn, D., et al, "*An analysis of thick-sample effects in the measurement of directional-hemispherical transmittance*" Optics Communications, vol. 118, no. 1, pp. 1–8, 1995

[15] DIN EN 410:2011